

Design criteria and recent developments of optical single particle counters for fossil fuel systems

Donald J. Holve
Daniel Tichenor
James C. F. Wang
Donald R. Hardesty
Sandia National Laboratories
Combustion Sciences Department
Livermore, California 94550

Abstract. Optical methods for particle size distribution measurements in practical high temperature environments are approaching feasibility and offer significant advantages over conventional sampling methods. The present paper begins by summarizing user requirements for research and on-line particle measurements in fossil fuel systems. The principles of single particle counter (SPC) design are outlined followed by a discussion of practical instrument design constraints. Three instrument design concepts currently being developed at Sandia are then discussed. An overview of these current methods and other instrument designs is presented with particular emphasis on capabilities to meet user objectives. Validation and long term testing of these new concepts is considered to be the final important step in achieving user acceptance of *in situ* optical counters.

Keywords: combustion and analysis; optical particle measurement; single particle counter; fossil-fuel systems.

Optical Engineering 20(4), 529-539 (July/August 1981).

CONTENTS

1. Introduction
2. User requirements
3. Design constraints for SPC instruments
 - 3.1. General principles of SPC design
 - 3.1.1. Response functions
 - 3.1.2. Dynamic range
 - 3.1.3. Sample volume
 - 3.1.4. Number density
 - 3.1.5. Resolution, accuracy
 - 3.2. Practical design constraints
 - 3.2.1. Illumination
 - 3.2.2. Light collection
 - 3.2.3. Windows
 - 3.2.4. Thermal effects
 - 3.2.5. Electronics
4. Recent SPC developments at Sandia
 - 4.1. Variable frequency grid technique
 - 4.2. Small-angle near forward scattering technique
 - 4.3. Intensity deconvolution method
 - 4.4. Combustor exhaust simulation facility for diagnostics evaluation
5. Capabilities and limitations of SPC concepts
6. Conclusions
7. References

1. INTRODUCTION

The design of rugged optical instrumentation for research studies and on-line monitoring of high temperature combustion flows remains a topic of current research interest. In particular, *in situ* measurement techniques for particle loading and size distribution can provide important data for the reliable design of combustion process equipment and control of environmental factors. Current and potential combustion applications include the study of

- Ash formation from pulverized coal
- Mineral carryover from fluidized bed combustors and pressurized gasifiers
- Droplet atomization and distribution in spray combustors
- Radiative heat transfer
- Boiler fouling
- Particle deposition in flow trains
- Soot formation
- Ash condensation.

An overview of diagnostics requirements for advanced power systems by Hardesty¹ clearly demonstrates the need for on-line continuous measurements of mass loading and size distribution. Two classes of advanced open-cycle gas turbine systems have been proposed for use in combined cycles for stationary power generation. In the first, the gas turbine will be combined with a multistage fluidized-bed combustor. The turbine operates directly on the cleaned, completely reacted combustion products from the pressurized fluidized bed. The temperature of the product gases at the inlet to the gas turbine is relatively low (e.g., ~ 1100 K). In the second system, the gas turbine

Invited Paper EP-102 received Mar. 23 1981; revised manuscript received Apr. 14, 1981; accepted for publication Apr. 14, 1981; received by Managing Editor Apr. 14, 1981
© 1981 Society of Photo-Optical Instrumentation Engineers.

has an integrated second-stage combustor which is fueled by cleaned, hot, low-Btu gas generated by a pressurized gasifier. The gas temperature at the turbine inlet approaches 1900 K.

The commercial acceptability of these advanced power systems will depend upon the efficiency, reliability, and longevity of the principal individual components, particularly turbine blades. Environmental constraints must be met by the integrated systems. In particular, the design of advanced coal-fired gas turbines will impose strict requirements on the flow characteristics at the turbine inlet. These requirements will in turn impose rigid standards of efficiency and reliability on the novel, high temperature gas cleanup systems, which are located upstream of the turbine inlet. In a recent workshop, Self² has summarized the availability of both sampling-type instrumentation and development of *in situ* optical systems for particle measurements in high temperature flows. The limitations of conventional techniques which use physical probes for measurements in gas turbines are well documented.³ Extractive sampling is limited by "...the general problem of obtaining a representative sample. Care must be taken to avoid biasing the distribution by nonisokinetic sampling and by size-dependent loss of particles in flow lines and dilution quenching devices. Extractive sampling from high temperature and high velocity flows^{4,5} poses additional problems since quenching of the flow for input to an external instrument may result in further condensation of water and mineral vapors."²

In situ optical sizing techniques offer great promise of alleviating many of the above limitations although detailed chemical analysis will continue to require extractive sampling. However, optical methods have not yet achieved sufficient reliability to be considered as standardized instruments, and in fact are presently limited in their size range capability, maximum number density, operational simplicity, and high cost.

Optical methods can be characterized as imaging or light scattering. Both methods can be further subdivided into ensemble or single particle techniques. Because of the need for spatial resolution, real time analysis, and mass resolution (mass is concentrated in the upper end of the size distribution) in many conventional and advanced power systems, our work at Sandia and the emphasis of this paper is directed to development of an optical single particle counter (SPC). Hirleman has recently reviewed the relative advantages and applicability of various SPC concepts.⁶ The present discussion is intended to complement Hirleman's review with primary emphasis on user needs and implications for practical SPC design.

The objectives of the present paper are to

- (1) summarize the ideal requirements of any SPC method for application in current and future power generation applications;
- (2) characterize the general principles and design constraints of an SPC instrument, consistent with (1);
- (3) summarize several development concepts being pursued at Sandia National Laboratories, Livermore;
- (4) compare capabilities of primary SPC concepts with user needs, and;
- (5) discuss validation requirements for demonstrating successful instrument design.

2. USER REQUIREMENTS

Table I summarizes typical user requirements for an SPC instrument. Both number and mass densities are required for adequate process and environmental control. If assumptions are made about the material density, the mass loading can be derived from the number density distribution. Previous specifications for process equipment have been based on mass loading measurements, since detailed distribution measurements have been tedious if not impractical to obtain. However, it is unclear whether a total mass loading specification is meaningful; indeed, it has been found that allowable mass loadings increase with a reduction in maximum particle size,¹ indicating that the number density distribution might be a more useful criterion when an SPC instrument is routinely available.

The sizing range required for adequate process control probably

TABLE I. User Requirements for SPC Instruments

Measurement Objectives	Typical Operating Conditions
1. Maximum Number Density	$10^4 - 10^6 / \text{cm}^3$ at $1 \mu\text{m}$
2. Particle Size Range	$0.1 - 100 \mu\text{m}$
3. Insensitivity to Particle Complex Refractive Index, n_2	$0 \leq n_2 \leq 1$
4. Insensitivity to Particle Shape	Length: Width $\leq 2, 1$
5. Particle Velocity	$1 - 100 \text{ m/s}$
6. Insensitivity to Temperature	Up to 2000 K
7. Insensitivity to Pressure	Up to 20 atm
8. Maximum Working Space Between Optical Elements	$0.5 - 2 \text{ m}$
9. Spatial Resolution	$0.5 - 5 \text{ mm}$
10. Minimum Measurement Time	10s; Depends on Particle Number Density

has a lower bound of $0.1 \mu\text{m}$, though soot formation and ash condensation effects would require monitoring down to $\sim 0.01 \mu\text{m}$. However, in all likelihood the practical limit of single particle counting in high number density flows is about $0.1 \mu\text{m}$ as discussed in Sec. 3.

Minimum sensitivity to particle refractive index ($\bar{m} = n_1 + n_2$), and particle shape variations is desirable in coal-fired flows where particle properties range from irregularly fractured carbon particles ($n_2 \approx .5$) to fused silica fly ash ($n_2 \approx .001$). Liquid fuel droplets are in general transparent ($n_2 \approx 0.0$) and spherical. If particle properties and shapes are known and invariant, these restrictions on instrument design become less stringent.

Wide velocity, temperature, and pressure ranges introduce additional design constraints on optical and electronic instrumentation. Large optical path lengths increase alignment errors and cost of the optical design. Finally, SPC instruments excel in providing spatially and temporally resolved size distribution measurements.

There are additional nonquantitative user requirements for a successful SPC instrument. The instrument must be rugged to withstand harsh mechanical and thermal environments without requiring frequent recalibration, and for on-line use, relative ease of operation is an imperative. Keeping these general requirements in mind, the following section discusses in more specific detail the criteria for SPC instrument design.

3. DESIGN CONSTRAINTS FOR SPC INSTRUMENTS

Although most discussions, and indeed technical papers, refer to particle measurements as "particle sizing," it would be more correct to say "particle size distribution" measurements. Measurements of particle size alone, without accurate counting of the number in each size class, would not provide meaningful information for characterizing mean diameters (number, area, mass) or integrated values of the properties, all of which are necessary for quantitative characterization of high temperature two-phase systems. This may appear to be an obvious and trivial point, but it is fair to say that many discussions have emphasized accurate size characterization with limited discussion of proper number counting. In practice, accuracy of frequency distribution measurements and derived averages is equally dependent on sizing and number counting accuracy. With this emphasis in mind, the following discussion describes the basic relationships constraining the design of single particle optical counters.

3.1. General principles of SPC design

Figure 1 shows a schematic diagram of a single particle counter and sizer with symbols indicating the primary instrument design variables. Typically, a laser of wavelength λ and beam f-number F_β is

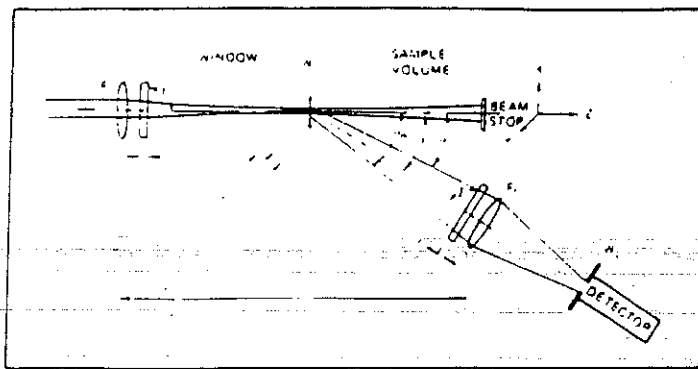


Fig. 1. General configuration for an optical single particle counter (SPC).

focused through a window of thickness t and angle γ to a beam waist W_0 . Scattered light from particles of velocity U_y is collected by a lens of open aperture $(\theta_1 - \theta_0)$ or f -number F_c at an angle θ and focused onto a detector slit assembly of width W_s . The available working space between the two lenses is denoted by L . The sample volume from which scattered light is detected is determined by the intersection of the beam focus and image of the slit. The single particle signatures at the detector are electronically and/or numerically processed to provide size frequency distributions.

The basic expressions relating signal amplitude, particle size, sample volume intensity distribution, and number density are summarized in Table II. The key points regarding each expression are discussed in detail in the remainder of this section.

TABLE II. Fundamental Relations for SPC Design*

1a. Scattering Amplitude, and	$A_j = \beta_1 \cdot I(x, z) \cdot F(d_j, \bar{m})$
1b. Response Functions	$F(d_j, \bar{m})$ or $R(d_j, \bar{m})$
2a. Signal Dynamic Range, and	$D_1 = A_m/A_t = I_m/I_t = F(d_m, \bar{m})/F(d_t, \bar{m})$
2b. Size Dynamic Range	$D_2 = d_m/d_t$
3a. Maximum Sample Volume, and	$V_m = \beta_2 \left(\frac{p}{p+1} \right) \frac{W_0^2 W_s}{\sin \theta} \left\{ \frac{1}{2} \ln(n D_1) \right\}^{p/(p-1)}$
3b. Cross Section for Particle Size d_j	$S_j = \beta_3 \frac{W_0 W_s}{\sin \theta} \left\{ \frac{1}{2} \ln [F(d_j, \bar{m})/F(d_t, \bar{m})] \right\}^{(p-2)/2p}$
4a. Cross Section Weighted Number Density, and	$n_j = C_j/U_j S_j$
4b. Maximum Number Density	$N_{max} = \sum n_j \leq 4P_s/V_m$
5. Resolution, Counting Uncertainty Due to Number Statistics	$ \Delta C_j/C_j _{95\%} = 2/(C_j)^{1/2}$

*Nomenclature defined in text.

3.1.1. Response functions

There are two basic methods of relating particle size to a scattering signal. The first approach is based on absolute scattering and gives the measured scattered light amplitude A_j as a function of a gain constant β_1 , the local illumination intensity in the sample volume $I(x, z)$, and the absolute response function $F(d_j, \bar{m})$,

$$A_j = \beta_1 \cdot I(x, z) \cdot F(d_j, \bar{m}) \quad (1)$$

The absolute response function is dependent on particle diameter, d_j , and complex refractive index $\bar{m} = n_1 + in_2$. In this method the intensity must be known or some method must be devised to account for sample volume intensity variation. The second type of response function $R(d_j, \bar{m})$ is the ratio of two independent absolute scattering signals from the same particle. The advantage of the ratio method is that it eliminates the need to determine the local particle illumination

intensity. The subscript j refers to a discrete amplitude or size class. Although ratio methods characterize particle size independently of the illumination intensity, the absolute magnitude of each ratio signal depends on the local illumination intensity and absolute response function.

Examples of absolute scattering techniques compared to scattering ratio methods have been described in Ref. 6. Scattering ratio methods include the angle-ratio technique⁷ where the scattered light intensity at two or more angles is ratioed, and the laser-Doppler velocimetry (LDV)-visibility method⁸ where the visibility ratio is an amplitude-normalized scattering signal. Examples of response functions for both methods are shown in the top half of Fig. 2, where the dashed curves refer to the angle ratio method with associated scattering angles, and the solid curve characterizes a typical visibility response curve with fringe spacing, δ . These response curves tend to be multivalued, either limiting the dynamic range or requiring multiple angle ratios to determine which of the multiple function values applies.

The lower half of Fig. 2 shows typical absolute scattering response curves for both absolute scattering and scattering ratio methods. For the angle ratio method and the SANFS method (described in Sec. 4.2), the dashed curves give the absolute signal response for annular light collection at specified angles, θ , and associated differential angles, $\Delta\theta = \theta_0 - \theta_1$. Response curves for the differential angle light collection have increased sensitivity, but require increased dynamic range capability from the detector. The multivalued response also limits the useful range and sizing capability for each angle, θ . The solid response curves apply to both absolute scattering and visibility methods which use an off-axis collection lens with $\theta_1 = 0.6^\circ$ and $\theta_0 = 15^\circ$.

For nonabsorbing particles ($n_2 = 0$), the absolute scattering curve

shows multivalued resonances which reduce the sizing resolution for some values of $\alpha (= \pi d/\lambda)$. Resonances also occur for the ratio methods (not shown in upper part of Fig. 2), similarly reducing their sizing resolution. The effect of absorption ($n_2 \geq 0.1$) is to smooth all response curves, giving a single-valued response function.

All the response functions shown in Fig. 2 have been evaluated for near-forward scattering angles, θ_1 , which provide minimum sensitivity to variations in n_2 and particle shape.⁹ Note that even for $\theta_1 = 0.6^\circ$, for $\alpha > 150$ some roll-off in the response function for absorbing particles compared to transparent particles is predicted and must be taken into account. Far off-axis light collection is unsatisfactory unless n_2 is a known quantity.

3.1.2. Dynamic range

The required signal dynamic range of the electronics

$$D_1 = A_m/A_t = I_m/I_t = F(d_m, \bar{m})/F(d_t, \bar{m}) \quad (2)$$

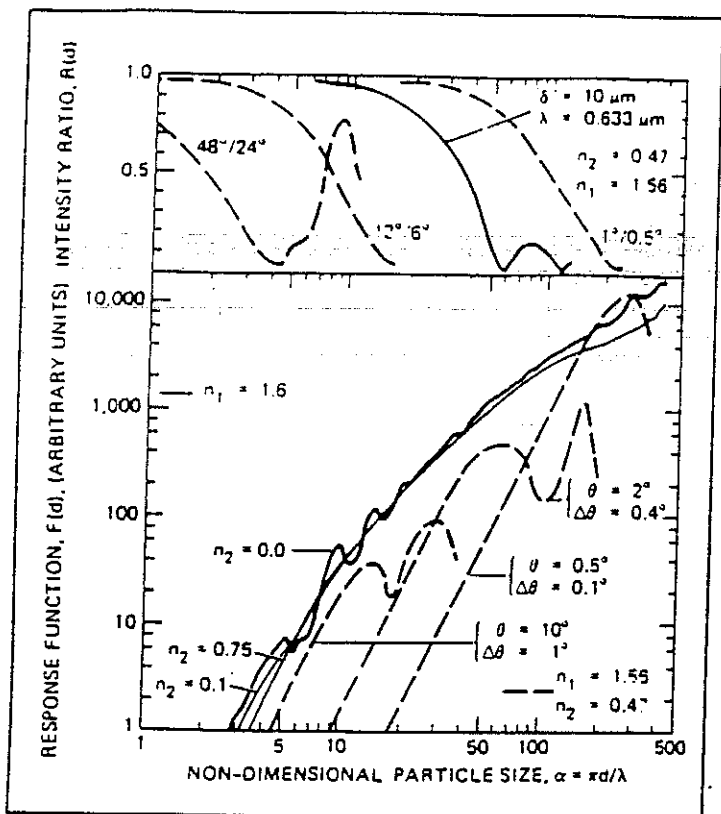


Fig. 2. Comparison of response functions for ratio and absolute scattering methods. The response curves for 12°/6° and 1°/0.5° have similar oscillations after the first minimum (not shown) as the 48°/24° curve.

is determined by the absolute response function $F(d_j, \bar{m})$ for both the scattering ratio and absolute scattering methods where the subscripts m and t refer to the maximum and threshold values, respectively. The value of D_1 thus determines threshold intensity of the illumination beam, I_t , and minimum signal amplitude, A_t . For a given size range, methods which collect light over a large solid angle have higher threshold values and smaller signal dynamic range than those methods which collect light over a small differential angle (Fig. 2) where the required dynamic range for a factor of ten in particle size approaches 10^4 . In practice, the size dynamic range $D_2 (= d_m/d_t)$ of the angle ratio method is limited by the sensitivity of ratio response $R(d_j, \bar{m})$ of each angle pair.

3.1.3. Sample volume

The sample volume from which scattered light is detected is an important feature of all single particle counters. A schematic diagram of a quadrant of a typical sample volume intensity distribution is shown in Fig. 3. The term \bar{I} is a normalized intensity, and, for a given intensity level \bar{I} , the sample volume cross section S_j is shown projected onto the x - z plane (crosshatched region).

The maximum sample volume size at intensity level \bar{I}_t is given by

$$V_m \approx \beta_2 \left(\frac{p}{p+1} \right) \frac{W_o^2 W_s}{\sin \theta} \left(\frac{1}{2} \ln D_1 \right)^{\frac{p+1}{p}} \quad (3a)$$

and variation of sample volume cross section with particle size is expressed as

$$S_j \approx \beta_3 \frac{W_o W_s}{\sin \theta} \left\{ \frac{1}{2} \ln \left[\frac{F(d_j, \bar{m})}{F(d_t, \bar{m})} \right] \right\}^{\frac{p+2}{2p}} \quad (3b)$$

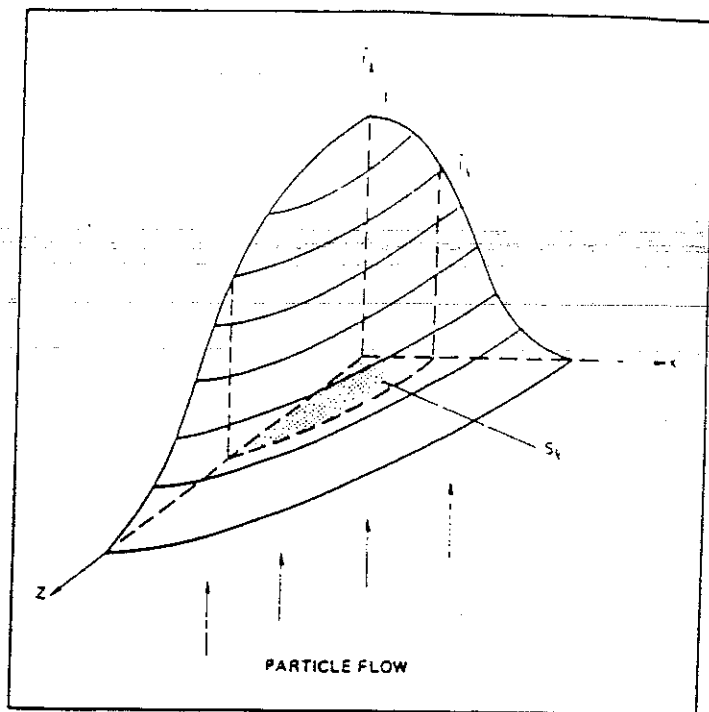


Fig. 3. Schematic diagram of a quadrant of the measurement volume intensity distribution $I(x, z, d)$ and cross-section area S_j associated with intensity level I_t .

These approximate expressions describing V_m and S_j were derived assuming a Gaussian beam focus convolved with a detector slit function profile which is determined by the blur spot size of the receiver lens (discussed later) relative to the detector slit width. The detector slit intensity profile can be reasonably approximated by an exponential expression, $\exp[-2(2x'/W_s)^p]$, where the power p is experimentally measured and the coordinate x' is at an angle θ to the coordinate x . Given this model for the measurement volume intensity distribution, the sample volume and intensity level cross sections can be integrated to give Eq. (3). The primary dimensions are mainly determined by the beam waist W_o , the detector slit width W_s , and effective light collection angle θ which decreases with increasing particle size for particles larger than $5 \mu m$. Of secondary importance are the power p (≥ 2) and the dynamic range D_1 . The cross-section area varies approximately logarithmically with particle size response function $F(d_j, \bar{m})$ where the log function is raised to a power ranging between 0.5 and 1.0.

Thus any sizing method, whether it be ratio or absolute scattering requires knowledge of the absolute scattering response function and sample volume intensity distribution to determine the variation of sample volume cross section with particle size. The reader should note that sample volume size and cross-section variation are significant features of SPC instrument design which directly influence the proper measurement of size-frequency distributions.

3.1.4. Number density

The need for knowing the variation in cross section S_j is illustrated by the expression for particle number density per unit volume in size class j .

$$n_j = (C_j / U_j \cdot S_j) \quad (4a)$$

The quantity C_j is the number of instrument counts per second in size class j , and U_j is the flow velocity of particles in size class j . Depending on the size resolution and dynamic range, S_j can differ by one or two orders of magnitude between the smallest and largest particle sizes of interest. Accounting for this sample volume cross-section bias is thus an essential feature of any SPC design.

An important constraint on any SPC instrument is the maximum number density in the flow that can be accommodated without having two or more particles in the same volume simultaneously. This limit is given by

$$N_{max} = \sum n_j \leq 4P_i / V_m \quad (4b)$$

where P_i is the probability of having two or more simultaneous scattering events in the sample volume. It is this constraint more than any other that will limit the lower size limit capability of SPC instruments for practical flows where number densities typically exceed 10^6 to 10^7 particles/cm³ for submicron particles.¹⁰ The requirement for a small volume dictates a small beam waist W_0 , which in turn makes it impossible to generate a uniform intensity sample volume at large focal lengths. Due to diffraction limitations with a practical lens f-number, it is the nonuniform intensity distribution that creates the additional problem of size ambiguity in absolute scattering methods (Eq. (10)), encouraging the development of optical methods. Nonuniform intensity also generates a variable sample volume or numerical discrimination cross section as a function of particle size. In short, the number density requirement is the central consideration in the successful design of an *in situ* SPC instrument.

3.1.5. Resolution, accuracy

The 95% confidence level uncertainty in the instrument count is given by

$$|\Delta C_j / C_j|_{95\%} \approx 2 / C_j^{1/2} \quad (5)$$

showing that 1000 counts or more are required for less than 6% uncertainty. This result is of particular concern when deriving mass-frequency distributions which are based on a small percentage of the total number distribution. Implicit in Eq. (5) is a tradeoff in size resolution. Greater size resolution (smaller size bin widths) implies fewer counts and thus increases uncertainty in the number count. Correspondingly larger size bin widths increase the number count accuracy. Other factors controlling size bin widths include amplitude conversion accuracy, multivalued characteristics of the response function, and optical alignment stability. Optimal precision in determination of the frequency distribution occurs when size and number uncertainties are equivalent.

3.2. Practical design constraints

Practical SPC design constraints are listed in Table III covering illumination, light collection, windows, thermal effects, and electronics. Similar to the previous format, the key points regarding each subject are discussed in detail in the remainder of this section. The symbols in Table III are defined in each discussion section.

3.2.1. Illumination

Specification of the beam waist diameter W_0 determines the beam depth of field Δz_b and maximum particle diameter d_m which experiences sufficiently uniform illumination. As shown in Table II, the number density requirement for a given application specifies the required sample volume size which in turn is determined primarily by the beam waist diameter. Figure 4 shows the impact of the number density limit on determining the operating range of an SPC instrument with, for example, a 30 μ m diameter beam waist and a light collection angle of 6°. The upper size range limit is controlled by near-uniform particle illumination, while the lower size limit boundary is specified by the size frequency distribution (assumed here to be $n_j \propto d_j^{-3}$) and reference cumulative number density. For low number density flows, the measurable size range increases, though at some lower size limit, signal-noise considerations will place an absolute lower limit on sizing capability. In practice, the cumulative number density above 1 μ m for coal-fired flows ranges from 10^4 to 10^7 /cm³¹⁰ giving a lower size range capability of 0.4 μ m for $W_0 = 30 \mu$ m. Although in principle the beam waist can be reduced to a few wavelengths of the illumination wavelength for small beam f-

TABLE III. SPC Design Constraints

1. Illumination	
• Beam Waist	$W_0 = 4F_b \lambda / \pi$
• 90% Depth of Field	$\Delta z_b = W_0^2 / 4\lambda$
• Uniform Particle Illumination	$d_m \leq W_0 / 4$
2. Light Collection	
• 90% Depth of Field	$\Delta z_c = 2F_c W_s$
• Image Quality, Blur Spot Size	$\Delta s \ll W_s$
• Spatial Filter Alignment	$\Delta x_c < \Theta \Delta z_b$
3. Windows	
• Axial Displacement	$\Delta z_w = \frac{N-1}{N} t$
• Lateral Displacement	$\Delta x_w = \gamma \frac{N-1}{N} t$
4. Thermal effects	
• Optical Table Thermal Expansion	$\Delta x_t = \alpha L$
• Refractive Index Distortion	$\Delta x_r \propto \epsilon L \frac{dT}{dy}$
• Background Radiation	Spectral Filtering Required
5. Electronics	
• Signal Dynamic Range	$D_1 = F(d_m, \bar{m}) / F(d_s, \bar{m})$
• Speed	$t \propto W_0 / U$
• Analog or Software Signal Validation, Discrimination	—

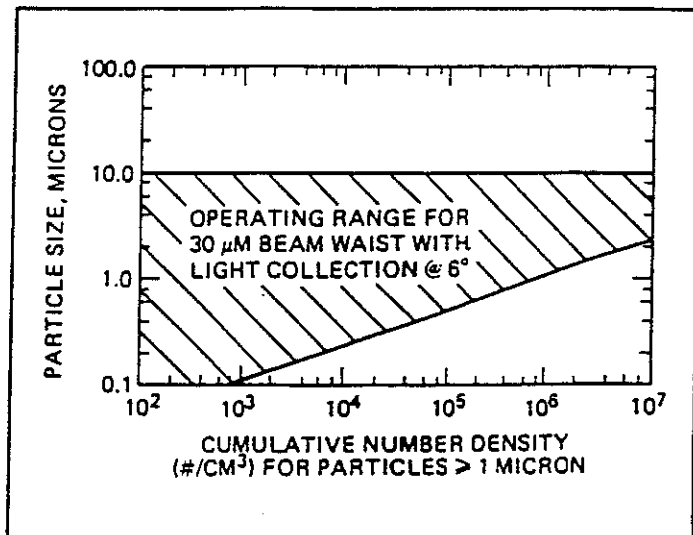


Fig. 4. Dynamic range of optical sizing instrument as a function of particle number density.

numbers, practical f-numbers increase with increasing focal length. Thus a smaller beam waist and higher number density capability will impose reduced working space, L . Plots similar to Fig. 4 can be determined for any chosen beam size. For example, a larger beam waist gives an increased upper bound on the particle size, while at the same time raising the lower bound. In fact, these results illustrate the need to use at least two beams of small and large beam focus to cover the submicron to 100 μ m particle size range.

3.2.2. Light collection

The depth of field of the receiver lens Δz_c is dependent on the receiver f-number, F_c , and the slit width at the detector, W_s . Because the sample volume intensity distribution is determined by the convolu-

tion of slit image space with the beam waist, stable alignment is best achieved if the image space of the slit is larger than the beam depth of field, Δz_b , and the blur spot diameter, Δs , of the receiver lens is much smaller than the slit width, W_s . In practice, for a high quality lens this can be achieved if the slit width is two or more times the beam waist, though the minimum slit width possible is desirable for maximizing number density capability.

If the above conditions are satisfied, lateral spatial filter alignment Δx_c is dictated by the beam depth of field Δz_b and light collection angle, θ . Although a maximum value of θ is desirable from this point of view and for maximum number density, minimum sensitivity to particle refractive index and shape is achieved for small θ , necessitating a tradeoff.

3.2.3. Windows

For measurements in duct flows, windows are a necessity and must increase in thickness, t , with increasing system pressure. Axial displacement of the focal volume is proportional to the window thickness and refractive index, N , while lateral displacement is additionally dependent on the incident angle, θ . For window thicknesses on the order of 1 cm, these displacements are large relative to the sample volume depth of field and thus require repositioning of the slit-detector when the instrument is mounted in place, or alternatively, calibration can be performed with equivalent windows inserted in the optical path. In addition, precautions must be taken to maintain relatively clean windows during measurements, though all instruments require a beam intensity detector to correct for any window obscuration or path length attenuation that occurs.

3.2.4. Thermal effects

For high temperature systems, thermal effects require consideration. Thermal expansion of the optical table Δx_t can be significant for large optical path lengths, L , giving a displacement of $25 \mu\text{m}/\text{m}\cdot\text{K}$ for aluminum and half this value for steel. For large L and hot environments, temperature control and/or use of an Invar mount may be necessary. Transverse temperature gradients in high temperature flows produce refractive index gradients which give beam pointing errors Δx_p , proportional to the optical path length L , transverse temperature gradient $(\partial T/\partial x)_t$, and axial distance ϵ over which the gradient occurs. For steady state duct flow systems, the probe beam is most likely aligned perpendicular to the flow and thus $(\partial T/\partial y)$ is parallel to the flow direction and probably minimal ($< 100 \text{ K}/\text{cm}$). For typical boundary layer thicknesses of $\epsilon \approx 1 \text{ cm}$ over which transverse gradients act, the resulting beam pointing errors are less than a few micro-radians, and thus of less importance than optical mount thermal expansion. For highly turbulent flows, temperature gradients and the turbulence scale may increase beam pointing errors to the point where the detector slit width must be increased. For high temperature systems, spectral filtering is required to block background radiation from surfaces and particles. Standard interference filters of 20 \AA half-widths have been shown to be adequate for this purpose.¹¹

3.2.5. Electronics

Detector-amplifier dynamic range, D_d , depends on the response function, $F(d)$, where the subscripts m and t in Table III refer to the largest and smallest particles, respectively. Required dynamic ranges for a tenfold size range vary from 500 for absolute scattering measurements to 10,000 for ratioing methods. Dynamic ranges of 10^4 require logarithmic circuits or staged amplifiers. Time response is not generally a problem, but for small particle measurements (requiring a small beam width) at high velocities, several hundred megahertz speed may be required.

Analog and/or software signal validation and discrimination are key elements in any successful instrument design, and generalizable guidelines are difficult to provide except for one: "the simpler, the better," both from accuracy and cost points of view.

In summary, for any SPC method, knowledge of two basic relationships are required: both absolute scattering and ratio methods

require knowledge of the response function $F(d, \bar{m})$, with knowledge of $R(d, \bar{m})$ as an additional requirement for ratio methods. Secondly, a relationship for the sample volume intensity distribution is required for characterizing the variation in sample volume cross section thus giving proper weighting of the number count density n_i with particle size. In theory, knowledge of the response functions alone would allow one to compute the sample volume cross section (Eq. (3b)), but the image quality of the light collection system is variable, requiring a calibration for the power p .

Table IV summarizes some of the design objectives and resulting tradeoffs that occur for any SPC system. The table is read as follows:

TABLE IV. Objectives and Tradeoffs for Design of Single Particle *In Situ* Sizing Instrument

	1	2	3	4	5	6	7	8
1. Minimize Lower Limit of Sizing Capability		0	-	-	-	0	+	0
2. Maximize Dynamic Range of Sizing	0		-	-	-	0	+	0
3. Maximize Optical Working Space	-	-		-	0	0	-	-
4. Maximize Number Density	-	-	-		-	0	0	0
5. Minimize Sensitivity to Particle Shape & Refractive Index	-	0	0	-		-	0	0
6. Maximize Sizing Accuracy	0	0	0	0	+		+	-
7. Maximize Optical Alignment Stability	0	0	-	0	0	+		-
8. Maximize Operating Temperature, Pressure	0	0	-	0	0	-	-	

Items 1-8 are primary, but, in some cases, competing objectives. The matrix is arranged to read the effects of numbered column objectives (same as row objectives) on row objectives designated by (+) for a positive effect, (-) for a negative effect, or (0) for a neutral effect. For example, satisfying objective (4) has a negative impact on achieving object (3). Additional independent objectives include velocity measurement capabilities for absolute number density evaluation (Eq. (4a)), and real-time analysis for monitoring of "upset" conditions. Finally, all of the above objectives are in conflict with cost minimization. Choosing between these objectives and selecting the best methods to achieve them remain as the primary topics of particle sizing research.

4. RECENT SPC DEVELOPMENTS AT SANDIA

Multiple-angle ratio counters, LDV-visibility methods, and several absolute scattering techniques have been described and compared previously.⁶ This section describes three methods currently under development at Sandia National Laboratories, Livermore, which emphasize different design objectives summarized in Tables I and IV. A diagnostics evaluation facility, which will be a key element in validating various instrument designs, is also described. Limitations and instrument design tradeoffs are discussed and then further amplified and compared with available SPC technologies in Sec. 5.

4.1. Variable frequency grid technique

In the LDV-visibility technique the particle interacts with a pattern having a single spatial frequency. An alternative to this approach is the variable frequency grid (VFG) technique, first suggested by Fristrom et al.,¹² in which the particle interacts with a pattern that contains a sweeping spatial frequency. In this system, Fig. 5, it is

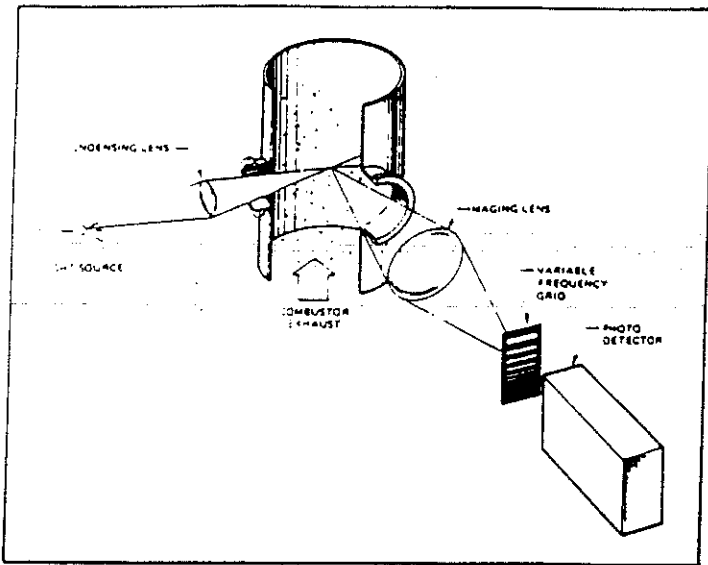


Fig. 5. Variable frequency grid technique for particle sizing (90° scattering arrangement).

more convenient to image the particle onto a grid rather than to cast a pattern of light and dark fringes into the sample volume. Since this technique is based on imaging, it is best suited for particles in the size range of 10 μm and larger. The following description summarizes current developments of the VFG method.¹³

The signal that contains the particle size information is generated by imaging the particle onto a grid and detecting the transmitted light. The grid consists of a series of alternately transparent and opaque parallel lines that decrease monotonically in width. It can be shown that the optimum grid is one in which the ratio of the widths of adjacent lines is a constant throughout the grid. As the image of the particle scans across the grid, the transmitted light signal becomes an oscillating signal modulated in both amplitude and frequency. The amplitude modulation, which depends on particle size, can be described in terms of a varying visibility function,

$$V(y) = 2 \left| \frac{J_1[\pi d / \Lambda(y)]}{\pi d / \Lambda(y)} \right| \quad (6)$$

where y is the position of the particle along the grid, J_1 is the first order Bessel function of the first kind, Λ is the local wavelength of the grid, and d is the particle diameter.

The first null in visibility occurs where the argument of J_1 equals 3.83. Given an optimum grid as described above, the particle diameter, d , can be expressed in terms of the number of oscillations, k , that precede the first null:

$$d = 1.22 \Lambda_0 R^{-k/n} \quad (7)$$

where Λ_0 is the local wavelength at the extreme low frequency end of the grid, R is the dynamic range (ratio of maximum to minimum Λ), and n is the number of line pairs.

In addition to size information, the velocity of the particle can be easily obtained by measuring the particle transit time through the entire grid. Since size and velocity of a particle can be measured simultaneously, velocity-size correlations are readily derived with the VFG method.

The VFG system is reasonably insensitive to particle shape. For irregular particles the dimension measured is approximately equal to the particle length in the direction normal to the grid lines. While the system is insensitive to the particle index of refraction, the particle must have a diffuse surface in order to be sized correctly. This condition is particularly important when coherent illumination is used. In general, white light illumination yields better signals for

nonideal particles. It may be possible to size specular particles by back lighting and operating the VFG system in a schlieren mode.

The VFG technique is particularly well suited to the measurement of incandescent particles (see Fig. 6) since no additional illumination of the particles is required. This feature may be useful in the study of pulverized coal combustion. In this application the system is not sensitive to the surface properties as long as the incandescence is more or less uniform over the particle. Mie scattering and LDV methods cannot utilize the particle incandescence in this manner.

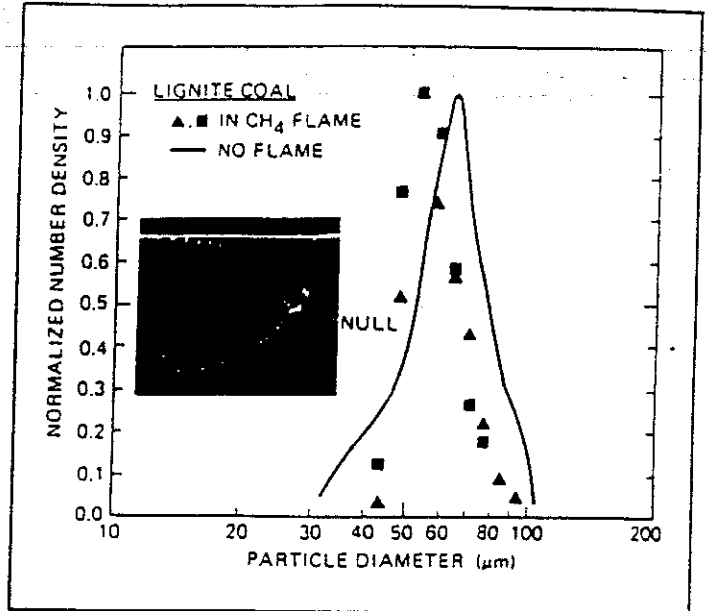


Fig. 6. Typical VFG response (insert) and sample VFG histogram of burning lignite coal particles.

4.2. Small-angle near forward scattering technique

The small-angle near forward scattering (SANFS) arrangement (Fig. 7) is configured to minimize refractive index and particle shape sensitivity in the response function.¹⁴ The method uses differential angle light collection at two angles, a small-angle collector to size the particle, and a large-angle collector to select particles to be measured.

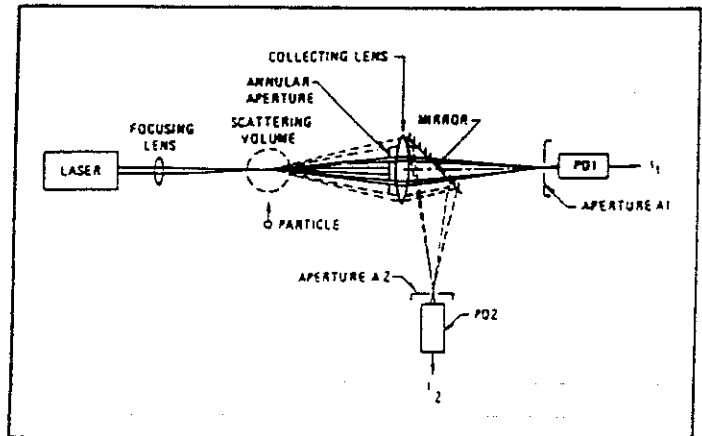


Fig. 7. Optical arrangement for the small-angle near forward scattering technique.

Light scattered by a particle in the forward small angles within the Fraunhofer lobe exhibits unique characteristics that are useful in particle size measurements. First, the scattering-intensity response versus particle size is a monotonic function instead of the oscillatory one at angles outside the Fraunhofer lobe. The monotonic behavior

of the scattering response at the small-angle near forward direction provides accurate size identification free from ambiguities inherent at large scattering angles. The second beneficial characteristic of the SANFS arrangement is the experimentally verified insensitivity of the scattering response within the Fraunhofer diffraction lobe to the refractive index of the particle.¹⁵

The scattered light response in the Fraunhofer lobe is also least sensitive to the shape of the particle. The effects of irregularly shaped particles can be approximated using the simpler Fresnel diffraction formula which shows that the intensity of the direct forward-scattered light is proportional to the square of the projected area of the particle. Of course, the direct forward-scattered light is obscured by the nondiffracted light, so that complete independence of the signal to particle shape cannot be achieved. However, the dependence on particle shape is minimized by collecting light at the smallest angles allowed by the nonscattered beam.

There are, however, tradeoffs associated with the SANFS arrangement as well. First, as with other Mie scattering techniques, it is important to accept only those particles that pass through the central region of the inspection volume. If a particle passes through the edge of the beam or if a particle is out of the focal plane of the collection lens, the response will indicate a particle smaller than the true size. These errors can be minimized by using the large-angle scattered light to determine when a particle passes through the central region of the sample volume (see Fig. 7). By choosing aperture A2 appropriately, the signal I_2 will be non-zero only when a particle passes through the central region of the beam. Since the depth of the field of the large-angle system is shorter than that of the small-angle system, the signal I_2 will be non-zero only when a particle is well inside the depth of field of the small-angle system. Edge effects and out-of-focus effects can be minimized by accepting only those pulses at I_1 that coincide with a pulse at I_2 . Figure 8 shows examples of calibration curves of the response functions of a typical SANFS arrangement. The solid curves are the calculated Mie scattering response

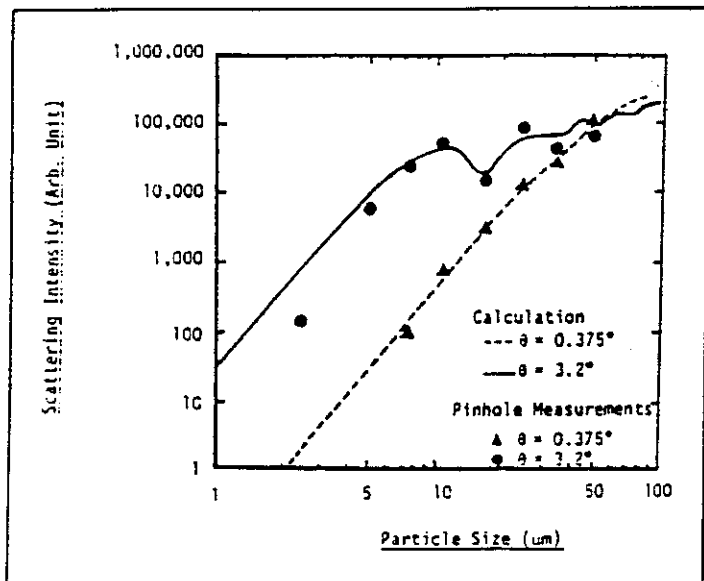


Fig. 8. Examples of a typical SANFS calibration curve (small angle at 0.375 degrees, large angle at 3.2 degrees).

functions. The symbols are the actual measured scattered light intensities using pinholes of known size at the sample volume. In principle, the effective scattering volume of the arrangement can be reduced to that of the large-angle coincidence collector. In a high-dust loading environment, only a small fraction of detected signals at the small-angle collector will be validated and measured.

There are inherent limitations of this arrangement which may be more or less severe depending on the application. First, the sample volume is larger with the SANFS arrangement than that achievable

with off-axis or large-aperture systems. Additionally, the optical discrimination method described above introduces further sample volume constraints. Therefore this system is most suitable for environments with particle density $\leq 10^2/\text{cm}^3$. Second, the pulse heights through much of the useful operating range are proportional to the fourth power of the particle diameter. For a tenfold dynamic range of particle size, a dynamic range of several thousands in the signal I must be handled by the electronics. Finally, the small collection annulus accepts only a small fraction of the total scattered light. This system may require a more powerful light source than that used with a large-aperture system. In applications where these limitations are not severe, the monotonic response and the insensitivity to particle shape and refractive index make the SANFS arrangement an attractive approach to particle sizing.

4.3. Intensity deconvolution method

The intensity deconvolution method^{11, 16} also uses near forward scatter (the optical geometry is similar to that in Fig. 1, with $\theta_i < 6^\circ$) to minimize refractive index and particle shape sensitivity, with the choice of inner angle light collection, θ_i , dependent on the size range of interest. The response functions for $\theta_i = 0.6^\circ$ are shown by the solid curves in Fig. 2. The optics and electronics discrimination in this method are simple because all scattering signals above a fixed threshold value, A_i , are accepted regardless of particle trajectory through the sample volume.

Because the scattered signal is trajectory dependent, a flow of monodispersed particles yields a signal peak amplitude count distribution having a sharp cutoff at some maximum signal value, corresponding to particles traversing the center of the measurement volume, with a spread to smaller amplitudes. To overcome this problem of nonuniformity of response within the measurement volume, a numerical inversion scheme, combined with a calibration procedure has been devised to unfold the distribution of signal amplitudes and yield an indicated size distribution which eliminates the dependence on trajectory. It is assumed that particles have an equal probability of passing through any element of the cross section, and that all particles have the same mean velocity, U , irrespective of size and trajectory.

The problem, then, is to devise a technique to unfold the measured signal amplitude count distribution in the presence of a nonuniform measurement volume intensity function $\bar{I}(x, z, d)$ to yield that which would be obtained with a uniform intensity function, and, hence, to obtain the true particle size distribution, $n(d)$. A set of equations relating experimental pulse height analyzer data $C_i(A_i)$, measurement volume function $\bar{I}(x, z, d)$, and the desired number distribution function $N(d)$ can be written in discrete form as

$$C_i = \sum_{j=1}^m U \Delta S_{ij} n_j, \quad i = 1, m \quad (8)$$

or in matrix form as

$$C = U \cdot \Delta S \cdot n$$

where

C_i = signal count rate for normalized signal peak amplitudes in a logarithmically scaled amplitude range, ΔA_i ;

n_j = concentration of particles in a logarithmically scaled size parameter range, Δd_j ;

and

ΔS_{ij} = cross-sectional area of the measurement volume normal to the flow direction, which yields normalized signal peak amplitudes in the range, ΔA_i , for particles in the size range, Δd_j .

The inversion of Eq. (1) is written symbolically

$$n = \frac{1}{U} \Delta S^{-1} \cdot C \quad (9)$$

Given the count rate distribution of signal amplitudes $C_i(A_i)$ in the pulse height analyzer channels, if the ΔS matrix is known, Eq. (2) can be solved to yield the number distribution $n_j(d_j)$.

The ΔS matrix is determined by passing a monodisperse particle distribution $N(d)$ of known diameter d_m and concentration n_m through the measurement volume at a known mean velocity U . Alternatively, Eq. (3b) in Table II can be used to compute ΔS if p has been determined. Once the ΔS_{ij} matrix elements are determined they are entered in the matrix inversion algorithm of a minicomputer. The solution n is derived by searching for a nonnegative vector n which minimizes the residual vector $R = C - U \cdot \Delta S \cdot n$. This procedure minimizes error propagation and also outputs values of residuals, which allows accuracy assessment of the resulting n_j distribution. Such calculations are straightforward and have been rapidly performed ($\leq 10s$) on a microcomputer.

Experimental results have been obtained for cold flow and burner flow conditions in the size range 2 to 30 μm , which compare favorably with independent Coulter counter measurements.¹⁶ More recent measurements have been obtained for burning pulverized coal in the size range of 4.0 to 80 μm , Fig. 9, which give good agreement with independent mass balances.¹¹ A dual beam-dual detector system

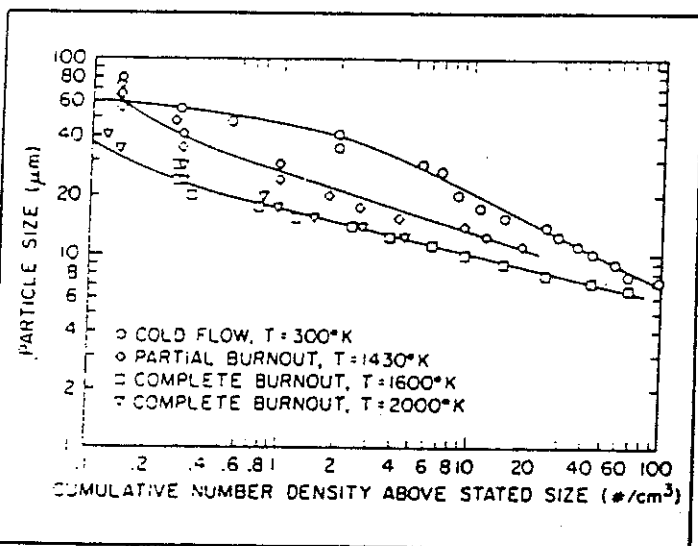


Fig. 9. *In situ* number density distribution for pulverized coal at four reaction temperatures.

(Fig. 10) is currently being fabricated for particle distribution measurements in the size range 0.3 to 80 μm with a maximum number density approaching $10^6/cm^3$ and working space of 0.6 m. The major limitations to this method are lack of particle size/velocity correlation and possible increased sensitivity to sample volume alignment errors, though current results indicate satisfactory performance.

4.4. Combustor exhaust simulation facility for diagnostics evaluation

The task of assessment and laboratory evaluation of advanced particle sizing diagnostic systems requires realistic testing environments which simulate combustor exhausts encountered in fossil fuel power systems. An atmospheric combustor exhaust simulation (ACES) apparatus has been built at Sandia. Except for pressure effects the device simulates the flow environment at the exit of an advanced fossil fuel combustor or at the turbine inlet and is a critically important test bed for advanced optical diagnostic techniques.

The ACES is shown schematically in Fig. 11. The combustor consists of (1) a dual-fuel burner which can burn both gaseous and

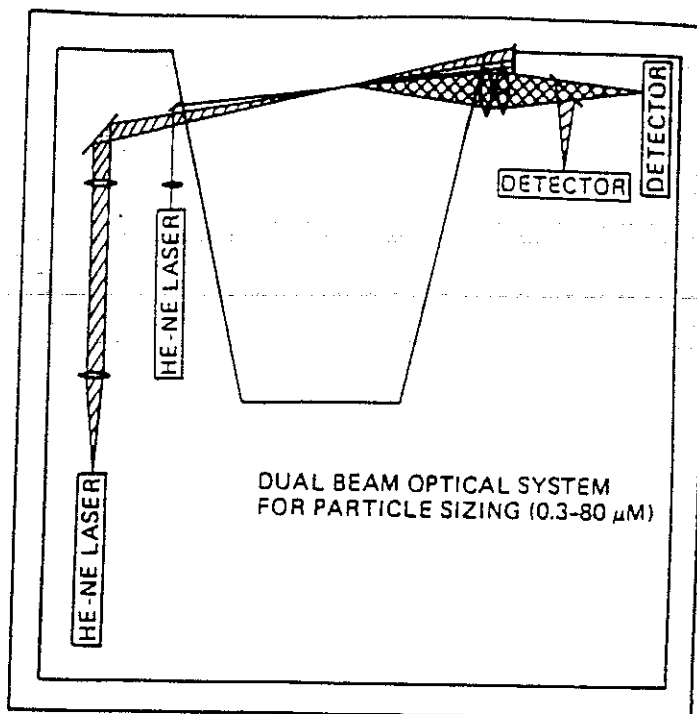


Fig. 10. Dual beam optical system for particle sizing (0.3-80 μm).

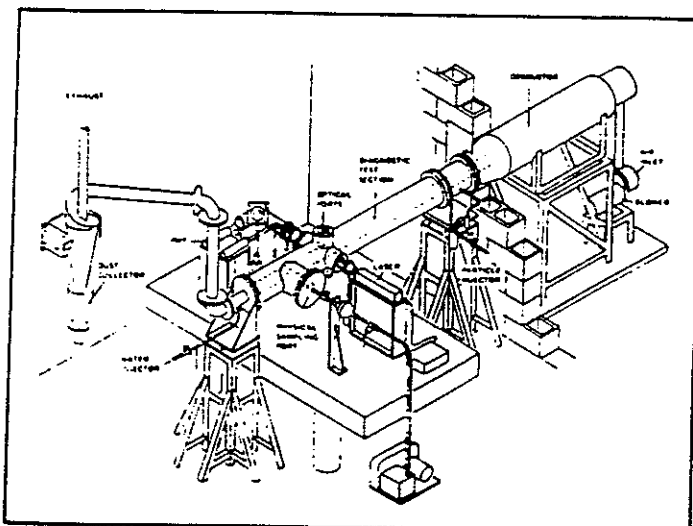


Fig. 11. Sketch of the atmospheric combustor exhaust simulator (ACES) facility.

liquid fuels and (2) a combustion chamber which provides a secondary air inlet downstream from the burner as well as a space to allow complete combustion. The mean exhaust temperature at the combustor exit can be controlled within ± 10 C from the set point between 500 and 1200 C with an automatic feedback temperature controller. The temperature profile across the test section which has a gas passage of 100 mm diameter was measured to be within 10 C of the mean value on the center line of the test section except near the wall.

Downstream from the transition pipe is the optical diagnostics test section which consists of four quartz windows of 50 mm in diameter each in the form of a "cross" perpendicular to the exhaust flow direction. The two windows in the two windows in the horizontal direction are designed as the laser inlet and the forward Mie scattering collection ports, respectively. The vertical set is used for the 90° Mie scattering as well as for other diagnostics access, e.g., in applications of spontaneous Raman scattering for gas temperature and species concen-

ration detection. An air purge is supplied to each window facing the hot gas path to maintain clean windows. Immediately following the optical section is a physical sampling tee-section which has an isokinetic sampling probe assembly mounted on the side flange. Measurement of the size distribution of the particulates collected by the sampling probe and that measured by an optical counter gives a direct performance comparison of the techniques. In addition, these instrument results can be compared with known particulate material and feed properties.

The operating characteristics of ACES are shown in Table V.

TABLE V. Operating Characteristics of Atmospheric Combustor Exhaust Simulator (ACES)

Pressure (atm)	1
Mean Temperature (C)	500-1200
Fluctuation Temperature (C)	2-10
Flow Rate(kg/min)	3-6
Velocity (m/s)	5-60
Particle Loading (g/m ³)	0-5
Particle Size Range (μm)	0.1-200

Constant mass feed rate of various particulate materials is accomplished by a fluidized bed feeder with stable feed rates exceeding twenty minutes duration. Typical particle material is derived from collected fly ash which has a mean diameter of 5 μm and a maximum diameter of 20 μm based on a Coulter counter analysis. A maximum feeding rate obtained with the present system is about 15 g/min which in a typical ACES flow corresponds to about 5 g/m³ particle density. The number density is in turn dependent on the chosen mean particle diameter.

This facility provides well-defined conditions for comparing various instrument concepts as well as for determining long-term alignment stability and robustness. We cannot emphasize too strongly the point that standardization and independent validation will be a key element in research and industrial application acceptance of optical SPCs and optical diagnostics in general.

5. CAPABILITIES AND LIMITATIONS OF SPC CONCEPTS

Hirleman's review⁶ has detailed the relative advantages and disadvantages of multiple angle ratio counters, LDV-visibility methods, and absolute scattering instruments. Briefly summarizing, all three basic methods have the capability of particle size measurements covering the submicron range to 100 μm or more. Sample volume size and thus maximum number density limits are determined primarily by the beam waist, light collection angle, and detector spatial filter. All methods are similarly subject to refractive index and particle shape uncertainties, though near-forward scattering minimizes sensitivity to these particle properties. The particle size dynamic range for a given light collection geometry is more restrictive for ratioing type counters (~8) than for absolute scattering methods (~15). All methods require use of dual illumination beams to cover the submicron to 100 μm size range. In addition, the ratioing schemes must use several angle ratios or fringe spacings to cover this wide size range (Fig. 2). All SPC methods are subject to the same statistical errors in number counting.

Many practical design constraints (Table III) are again general to all SPC methods. Visibility and some absolute scattering methods collect light over a relatively large aperture (F/4 lens) and thus have similar receiver characteristics, except for electronics speed requirements and signal validation and discrimination. Illumination techniques differ since the visibility method must use two overlapping beams to form a fringe pattern in the sample volume. Sample volume size limits are similar, though sufficiently accurate intersection of

two beam foci may be subject to thermal effects. Electronics speed requirements for visibility measurements in the submicron particle size range can approach 500 MHz for fringe spacings of 1 μm at velocities of 10 m/s. This is a factor of 30 higher than for absolute or multi-angle scattering methods with $W_0 = 30 \mu\text{m}$. Signal validation and discrimination for visibility measurements at 500 MHz have not yet been reported.

The multiple angle ratio method and the SANFS technique use single beam illumination but collect light at several small differential angles, $\Delta\theta$. The two angle concept gives two values for the depth of field (proportional to θ^{-1}), and thus sample volume cross section also differs by θ^{-1} . As a result, selection of scattering signals from the appropriate sample cross section through signal validation and discrimination is an important feature of these two methods. Because of a larger effective slit width (which also defines the differential light collection angle), the depth of field and sample cross section tend to be much larger for current multi-angle ratioing designs; as a result this reduces the maximum number density capability. Placing a spatial filter, W_s , at the image focus of the receiver lens allows reduction of the depth of field and sample volume. The differential angle could then be increased independently, giving increased signal levels. Although the SANFS approach solves the variable illumination intensity problem, it does so at the expense of requiring a larger sample volume, thus limiting its practical application to lower number densities.

The absolute scattering method with F/4 light collection and intensity deconvolution, described in 4.3, offers the greatest flexibility relative to the design constraints in Tables II and III. The primary questions for this method are the accuracy of the deconvolution procedure, and required optical alignment precision necessary for consistent results. Available results are satisfactory, but extension of this method to submicron applications will place more stringent alignment requirements on this technique. All SPC methods are subject to these alignment constraints, which become more severe with decreasing sample volume size. The estimates in Table III indicate feasible alignment accuracy for all methods, but actual experience with various SPCs is limited.

The VFG method is unique in that it offers some of the advantages of imaging techniques such as holography and photography, but provides the information in real time instead of requiring expensive and tedious off-line image analysis. Although the lower size range available to VFG measurements is theoretically limited by optical microscopy, it is best suited to particle sizes of 10 μm and larger.

Other desirable features for SPCs are velocity measurement capability, robustness, and reasonable production cost. Visibility methods have inherent capability to measure particle velocities, although, recently, simple transit timing methods have been demonstrated for single beam velocity measurements^{17,18} which are applicable to other sizing methods by the straightforward addition of standard nuclear instrumentation modules. Thus absolute number density evaluation is available to all sizing methods without modifying the optics or adding a separate velocity measurement method. Questions of robustness and reliability of particle analyzers will be answered by long-term testing on controlled exhaust simulation facilities. Cost considerations will ultimately dictate user choice between two or more feasible techniques.

6. CONCLUSIONS

In principle, several SPC concepts are feasible for obtaining *in situ* size distribution measurements in high temperature, two-phase flows with large optical working space. Various tradeoffs in capability of these instruments (Table IV) lead to a range of design options. Thus flexibility to modify instrument parameters to satisfy variable user requirements will be an important feature of practical instruments. The primary emphasis of current work on SPCs should be testing and evaluation of the various concepts under controlled but realistically simulated high temperature particulate flows. Instrument performance should be compared (where possible) with independent

standardized particle measurement techniques. With this emphasis in mind, current work at Sandia is proceeding with development of three measurement techniques and validation on an existing combustion exhaust simulator.

7. REFERENCES

1. Hardesty, D. R., ASME Papers No. 80-GT-129, presented ASME Gas Turbine Conference, New Orleans, March 1980.
2. Self, S. A., "Particle Measurements in High Temperature Flows," presented at National Science Foundation Workshop, Mississippi State University, September 1980.
3. Chedaille, J., and Braud, Y., *Measurement in Flames*, Vol. I of *Industrial Flames*, International Flame Research Foundation, Crane, Russak, New York (1972).
4. Symposium on Advances in Particle Sampling and Measurement, EPA, Ashville, NC, May 1978.
5. Tendulkar, S. P., et al., "High Temperature and High Pressure Sampling Devices for Particulate Collection in a Fluidized Bed Gasification Process," Reference 10, Volume IV.
6. Hirtleman, E. O., "Laser-Based Single Particle Counters for In Situ Particulate Diagnostics," *Opt. Eng.* 19(6), 854(1980).
7. Hirtleman, E. O., "Optical Technique for Particle Characterization in Combustion Environments: The Multiple Ratio Single Particle Counter," Ph.D. Dissertation, Purdue University, August 1977.
8. Farmer, W. M., *Appl. Opt.* 11, 2603(1972).
9. Moore, C., *J. Appl. Opt.* 17(19), 176(1978).
10. Schmidt, E. et al., *ATM. Envir.* 10, 1065(1976).
11. Holve, D. J., *J. Energy* 4(4) (1980).
12. Fristrom, R. M., Jones, A. R., Schwar, M. J. R., and Weinberg, F. J., *Faraday Symposia of the Chemical Society*, 7, 183(1973).
13. Wang, J. C. F., and Tichenor, D. A., *Appl. Opt.* 20(8), 1367(1981).
14. Wang, J. C. F., "Optical Particulate Size Measurements Using a Small-Angle Near-Forward Scattering Technique," SAND 79-8246, Sandia National Laboratories, Livermore, CA, July 1979.
15. Hodgkinson, J. R., *Appl. Opt.* 5, 839(1966).
16. Holve, D., Self, S. A., *J. Appl. Opt.* 18(10), 1632(1979).
17. Hirtleman, E. O., "Recent Developments in Non-Doppler Laser Velocimetry," AIAA 18th Aerospace Sciences Meeting, Pasadena, CA, January 14-16, 1980.
18. Holve, D., "A Transit Timing Technique for Velocity (Slowness) Measurements," Paper 80-49 presented at Western States Section/Combustion Institute, University of Southern California, Autumn 1980.